Review Article

CT and MRI of superficial solid tumors

Jingfeng Zhang[1], Yanyuan Li[2], Yilei Zhao[1], Jianjun Qiao[3]

[1]Department of Radiology, [2]Department of Pathology, [3]Department of Dermatology, the First Affiliated Hospital, College of Medicine, Zhejiang University, Hangzhou 310003, China

Correspondence to: Jianjun Qiao. Department of Dermatology, the First Affiliated Hospital, College of Medicine, Zhejiang University, No. 79, Qingchun Road, Hangzhou 310003, China. Email: qiaojianjun@zju.edu.cn.

Abstract: Superficial solid masses are common conditions in clinical practice, however, some of which can be easily diagnosed and others would be difficult. Although imaging of superficial masses is not always characteristic, it would be helpful to give a definitive diagnosis or narrow a differential diagnosis. Crossing-section imaging can depicture the masses directly, find some pathognomonic signs and demonstrate their relationship with adjacent structures, which can provide decision support for clinician's reference. Computed tomography (CT) can be used to detect calcifications and bone erosion which could not be seen on radiographs. Magnetic resonance imaging (MRI) is the preferred way for evaluating soft tissue lesions and provides information on hemorrhage, necrosis, edema, cystic and myxoid degeneration, and fibrosis. Other advantages of MRI are its superior soft tissue resolution and any profile imaging, which can aid the assessment of extension and adjacent infiltration. Positron emission tomography (PET)/CT and PET/MRI have been increasingly used in bone and soft tissue sarcomas and provides advantages in the initial tumor staging, tumor grading, therapy assessment, and recurrence detection. Therefore, imaging examination can play an important role in treatment decision making for superficial solid tumors. Here we review the important conditions presenting as superficial mass and show the imaging of typical cases diagnosed in our hospital.

Keywords: Computed tomography (CT); X-ray; magnetic resonance imaging (MRI); superficial; solid tumors

Submitted Jan 20, 2018. Accepted for publication Mar 06, 2018.
doi: 10.21037/qims.2018.03.03
View this article at: http://dx.doi.org/10.21037/qims.2018.03.03

Background

Superficial soft-tissue masses are common in clinical practice, and most of them are solid (1-4). Although they can be easily perceived, palpable and biopsied, radiological examinations are often used to assess their extension and depth of involvement, or to identify their relationship with the adjacent structures. Additionally, radiological examinations can depicture pathognomonic signs, such as fat components in lipoma or liposarcoma, or some specific signs to narrow differential diagnosis (3,5). Lesions that are assigned benign can be followed expectantly, whereas indeterminate or malignant lesions can be subjected to histological evaluation (1-3). Therefore, radiology can not only facilitate the diagnosis of superficial solid masses, but provide guides for treatment decision making.

The location of a solid mass within the superficial tissue is best described as cutaneous (epidermis and dermis); subcutaneous (adipose tissue, nerve tissue, fibrous tissue and vascular tissue etc.); or fascial (overlying the muscle) (4,6). Cutaneous lesions may be derived from the epidermis or dermis, and subcutaneous lesions may arise in the adipose tissue, or the fascia overlying the muscle (6,7). However, some lesions can invade the cutaneous and subcutaneous tissue simultaneously (4,6). For purposes of comprehensive understanding and analysis, it is most useful to categorize superficial soft-tissue solid masses by histology as skin appendage tumors, mesenchymal tumors and metastatic tumors.

Generally, most cutaneous tumors arising from the skin

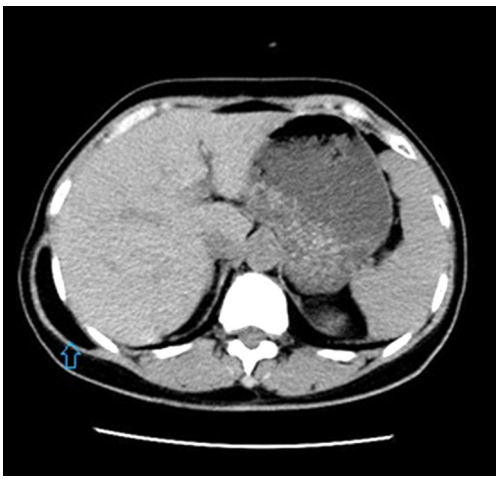

Figure 1 A 48-year-old female presenting with an encapsulated superficial lipoma intra-muscle of the right posterolateral chest wall. Axial unenhanced CT image shows a subtle mass (arrow) with attenuation identical to that of the subcutaneous adipose tissue.

appendage are easily seen and are liable to make a diagnosis accurately in the clinic, and metastatic tumors can also be easily diagnosed by clinical history, so imaging examination is limited (6). However, some large mesenchymal tumors arising from the cutaneous and subcutaneous tissue, especially with a malignant tendency, should be evaluated the area and depth pre-operatively. Current imaging techniques have markedly improved our ability to detect and diagnose these superficial soft tissue tumors (5,6,8,9). The anatomic location of lesions, the patient's age, imaging characteristics, and clinical manifestations should be taken into account for the differential diagnosis.

In this article, imaging features of a spectrum of histologically proven superficial soft-tissue solid mesenchymal tumors from our institution will be presented. It is intended as a comprehensive review with emphasis on relatively more common masses within the superficial soft-tissue, and the diagnosis may be suggested by radiological imaging especially magnetic resonance imaging (MRI). According to the 2013 version of World Health Organization (WHO) classification of soft tissue tumors, common superficial mesenchymal tumors will be presented in this article, including adipocytic tumors, fibroblastic/myofibroblastic tumors, pericytic/perivascular tumors, vascular tumors, nerve sheath tumors, and undifferentiated/unclassified sarcomas.

PET/CT has been increasingly used in bone and soft tissue sarcomas and provides advantages in the initial tumor staging, tumor grading, therapy assessment, and recurrence detection (10,11). PET/MRI may indeed provide greater accuracy than the currently available imaging procedures in the staging and later therapeutic response evaluation in soft tissue tumors (12,13).

In this paper, we mainly review the imaging characteristics on CT and MRI of superficial soft tissue tumors.

Adipocytic tumors

Adipocytic tumors are quite common and represent the largest single group of mesenchymal tumors (14). Lipoma is the most common benign adipocytic tumor, and liposarcoma is its malignant contrariety (14).

Lipoma

Lipoma is the most common soft tissue tumor in adults and is most frequent between the ages of 40 and 60. Superficial lesions are much more common than deep lesions. Lipoma is usually solitary, and approximately 5% of patients have multiple lesions. Most lipomas are small, 80% of which are less than 5 cm (6). Patients with superficial lipomas usually present with slowly growing subcutaneous soft tissue mass. Lesions are most commonly located on the trunk, shoulder, upper arm, and neck. Lipomas are usually asymptomatic, although the local pain, tenderness, and compression of peripheral nerves present in up to 25% of patients (14,15).

On CT and MR imaging, lipoma appears as homogeneous density or signal similar to that of subcutaneous fat. Thin fibrous septa are occasionally seen (16). Fatty components are pathognomonic for lipomas. On CT scanning, a lipoma demonstrates a homogeneous low attenuation with approximately –65 to –120 HU. Comparison of the tissue attenuation of tumor to that of surrounding normal fat is more reliable for diagnosis than an absolute CT value (*Figure 1*). A lipoma does not have discernible enhancement following the intravenous administration of contrast medium. When a lipoma is encapsulated, a surrounding fibrous capsule of low signal intensity on MRI may be delineated (*Figure 2*) (6,17). Alternatively, the capsule of a superficial lipoma may not be present or may be too thin to be perceived on imaging studies. On occasion, superficial lipomas may be difficult to distinguish from the adjacent adipose tissue. Comparison with the contralateral side can also be useful to identify subtle focal asymmetry (6). However, when a mass is with fat components and heterogeneous texture, a liposarcoma should be suspected.

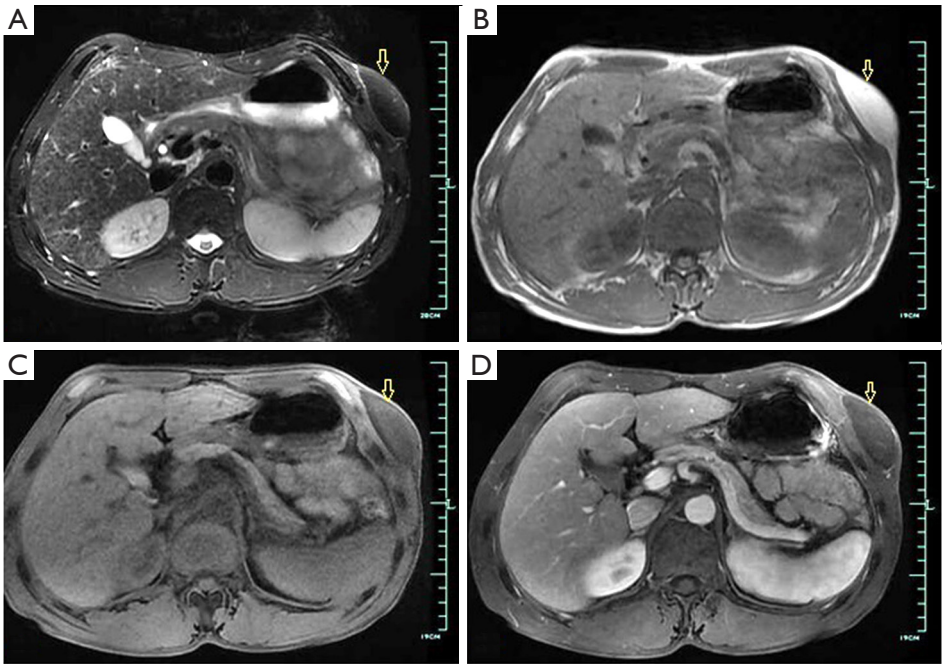

Figure 2 A 52-year-old female presenting with an encapsulated superficial (subcutaneous) lipoma in the left upper abdominal wall. (A) Axial T2WI with fat suppression displays a mass of fusiform shape with low signal along the subcutaneous tissue of the left abdominal wall (arrow); (B) axial T1WI shows high signal intensity homogeneously (arrow); (C) axial T1WI with fat suppression displays that the signal of the lesion decreases markedly (arrow); (D) axial T1WI after intravenous administration of gadolinium shows no enhancement in the mass (arrow).

Liposarcoma

Liposarcoma is the second most common soft tissue sarcoma with a variety of clinical presentations (18). Correspondingly they have a wide spectrum of imaging appearances that reflect its histologic heterogeneity, ranging from lesions nearly entirely composed of mature adipose tissue to those with very sparse fatty elements (18,19). In cases with fatty tissue in the masses, a diagnosis could be easily made (16). However, it is not achievable in other cases without fatty tissue in lesions. For radiological diagnosis, it is useful to separate well-differentiated from poorly differentiated liposarcoma in groups (16). Well-differentiated liposarcomas often display a predominantly fatty mass, with irregular, thickened, linear, swirled, and/or nodular septa (16,20,21). Myxoid and pleomorphic lesions usually show less fat and more heterogeneity (*Figure 3*) (21).

Fibroblastic/myofibroblastic tumors

Fibroblastic/myofibroblastic tumors are a heterogeneous group of neoplastic lesions in clinical practice and are seen in all age groups. The superficial types of these tumors mainly include benign (nodular fasciitis, elastofibroma, desmoplastic fibroblastoma), intermediate, locally aggressive (palmar/plantar fibromatosis), and intermediate, rarely metastasizing [dermatofibrosarcoma protuberans (DFSP)].

Benign fibroblastic/myofibroblastic tumors

Nodular fasciitis

Nodular fasciitis is a self-limiting benign fibrous neoplasm that usually occurs in subcutaneous tissue, which is composed of uniform fibroblasts or myofibroblasts (22,23). Nodular fasciitis primarily affects young adults (20 to 40 years of age) without a sex predilection. The upper extremity is the most frequently involved site, particularly the volar aspect of the forearm, followed by the lower extremities, head/neck, and trunk (22). Lesions may grow rapidly, initially suggesting an aggressive tumor. Lesions are typically subcutaneous and present as subcutaneous nodules, attaching to superficial fascia, although deeper locations may be affected. Mild pain or tenderness may be present in approximately 50% of cases. Complete excision is usually curative (23).

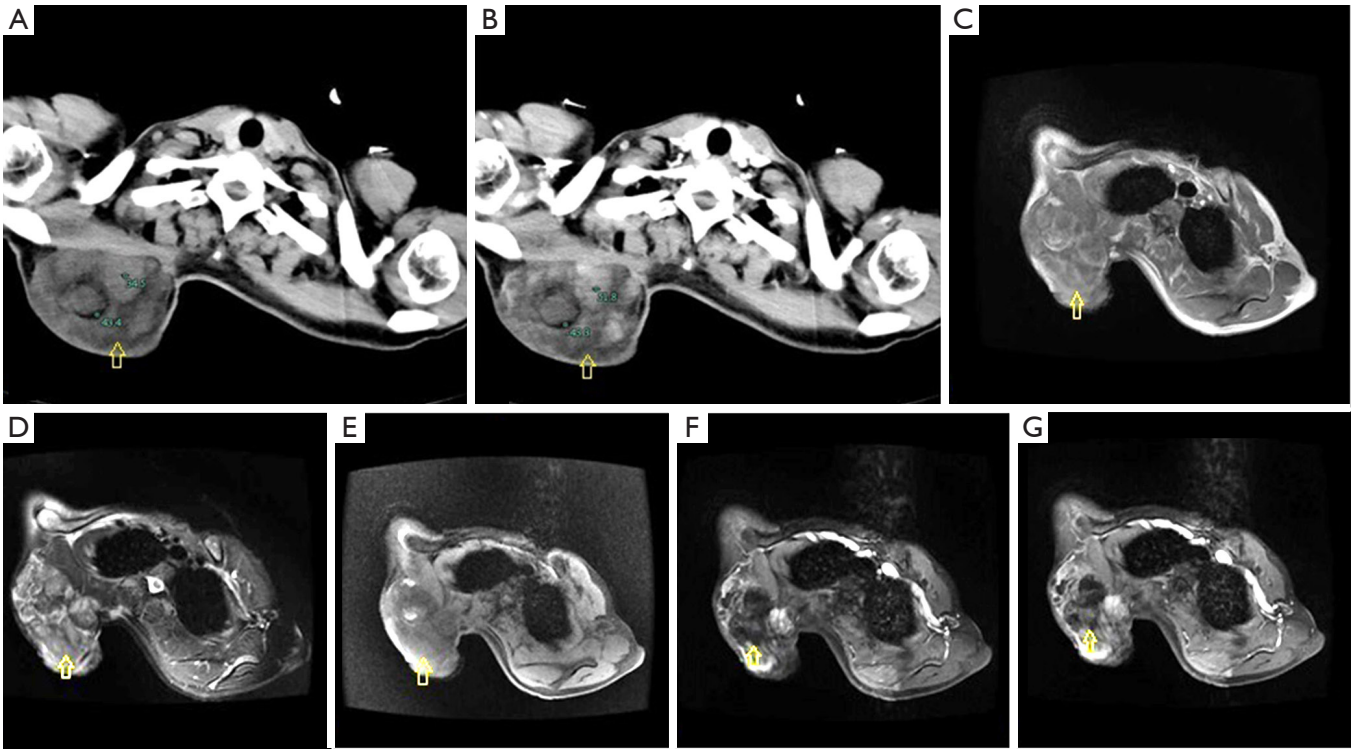

Figure 3 A 38-year-old woman with a superficial (subcutaneous), myxoid and pleomorphic liposarcoma involving the right shoulder back. (A) Unenhanced axial CT image shows ill-defined margins of tumor with fat attenuation as well as irregular zones with intermediate soft tissue attenuation (arrow); (B) contrast enhanced CT image shows marked heterogeneous contrast enhancement within the tumor and scattered unenhanced areas reflecting necrosis and myxoid components (arrow); (C) axial T1-weighted image and (D) conventional T2-weighted image with fat saturation demonstrate a large mass in the right shoulder back with predominantly mixed signal intensity on T1-weighted and T2-weighted images (arrows); (E) scattered areas within the mass show increased signal intensity on T1-weighted image with fat saturation due to subacute hemorrhage; (F,G) after intravenous administration of Gd-DTPA, the lesion is markedly heterogeneous enhancement on axial enhanced T1-weighted images with fat saturation. Some unenhanced areas within the lesion suggest necrosis and myxoid components.

The radiological description of nodular fasciitis is limited in the literature. Lesions may be ill-defined or well-defined on CT, with soft tissue attenuation similar to or mildly less than that of skeletal muscle (24-26). Subcutaneous lesions are frequently well-defined, delineated by the surrounding fat. MR imaging shows nonspecific low-to-intermediate signal intensity on T1WI and an intermediate-to-high signal on T2WI, with moderate to marked diffuse enhancement after intravenous administration of contrast medium (24-26). An important diagnostic feature at MRI is the linear extension along the superficial fascia (fascial tail sign), and mild surrounding edema may be seen on MR images (*Figure 4*) (24,27).

Elastofibroma

Elastofibroma is a benign, ill-defined proliferation of elastofibrous tissue characterized by an excessive number of abnormal elastic fibers (28). It occurs mostly in the elderly, with a peak incidence between the seventh and eighth decades of life. There is a striking predominance in females (28). Elastofibroma mostly occurs in a periscapular location, related to the scapular tip (29), and may be bilateral in some cases (28,30). On CT and MR imaging, the periscapular masses often contain small amounts of entrapped fat with otherwise nonspecific features. MR images frequently reveal intermediate signal intensity on T1WI and T2WI (29-31). The location and imaging appearance with entrapped fat is pathognomonic of elastofibroma (*Figure 5*). Elastofibroma has a characteristic location (infrascapular and periscapular region, deep to serratus anterior and latissimus dorsi) and a specific imaging appearance allowing accurate prospective

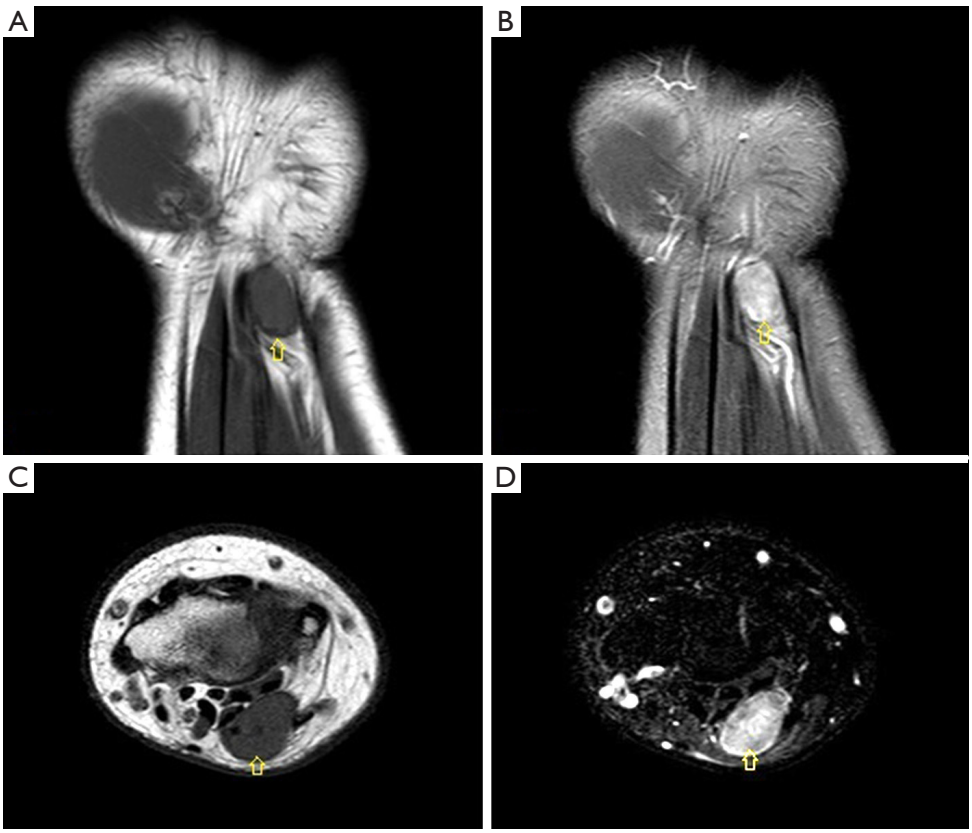

Figure 4 A 20-year-old woman with nodular fasciitis involving the wrist. (A) Coronal T1WI, (B) coronal T2WI with fat saturation, (C) axial T1WI, and (D) axial T2WI with fat saturation show a subcutaneous oval heterogeneous mass lying to the palmar carpal canal, with intermediate signal on T1WI and moderately high signal on T2WI (arrows). There is mild surrounding edema and fascial extension. The higher signal centrally on T2WI suggests the necrosis.

diagnosis. These lesions are bilateral in up to 60% of cases and when unilateral are more often seen on the right than left. The diagnosis of elastofibroma is readily established by typical anatomical location at the lower pole of the scapula and the clinical symptom of a scapular clunk as the arm is abducted or adducted (29-31).

Desmoplastic fibroblastoma

Desmoplastic fibroblastoma is a benign, paucicellular, soft tissue tumor with abundant collagenous or myxocollageneous matrix, low vascularity, and scattered, stellate-shaped and spindled fibroblastic cells (32,33). It usually affects patients in the fifth to seventh decades of life (70% of cases) and is more frequent in men. Lesions are most common in the subcutaneous tissue of the upper extremity, followed by the lower extremity, head/neck, back, and feet. More than 50% of lesions are larger than 5 cm (32-34). Desmoplastic fibroblastoma is a well-circumscribed, white to gray, subcutaneous mass, although infiltration of the surrounding fat, superficial fascia and muscle. Imaging findings of desmoplastic fibroma are described in only a limited number of case reports (34). MR imaging reveals prominent low signal intensity on all pulse sequences (*Figure 6*), due to hypocellular collagen. Only mild contrast enhancement is seen, which is in marked distinction from the majority of fibromatoses (34,35).

Intermediate-locally aggressive fibroblastic/myofibroblastic tumors

Palmar/plantar fibromatoses are fibroblastic proliferations that arise in the palmar or pantar soft tissues and are characterized by infiltrative growth. In general, small lesions that usually arise from fascia or aponeurosis (36,37). These lesions are typically slowly growing, in sharp contrast to the deep fibromatoses that usually grow rapidly and are larger

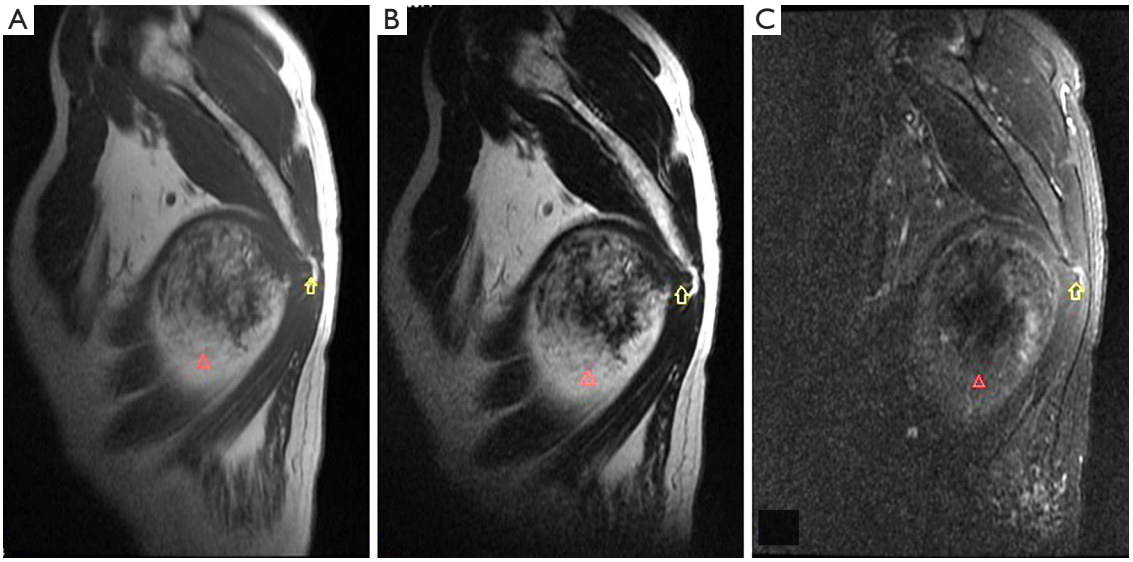

Figure 5 A 57-year-old man with elastofibroma involving the right periscapular location. (A) Sagittal T1WI, (B) sagittal T2WI, and (C) sagittal T2WI with fat saturation show a subcutaneous, ill-defined, oval heterogeneous mass, which is related to the scapular tip (arrows), with irregular low signal areas (means to fibrous tissue) inside the mass on both T1WI and T2WI, and small amounts of entrapped fat as well (arrow heads).

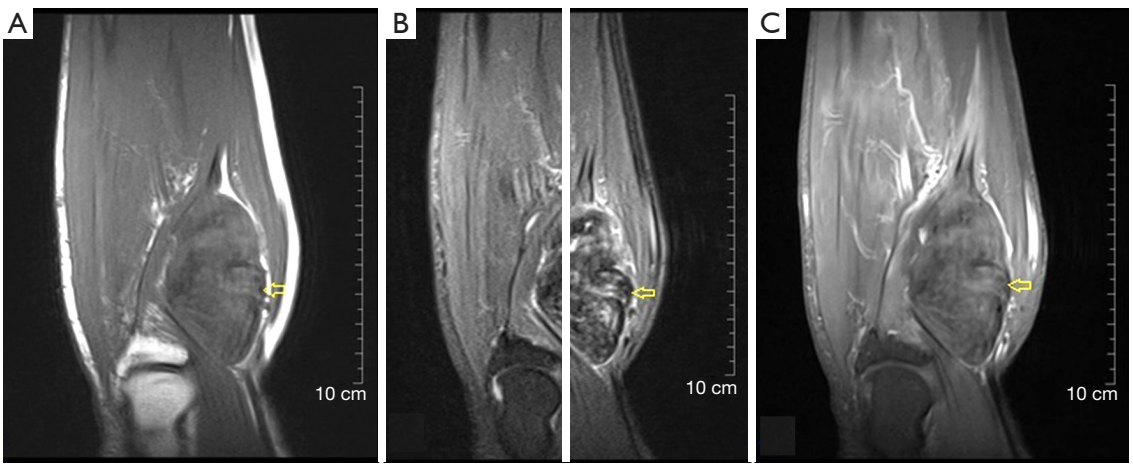

Figure 6 A 72-year-old woman with desmoplastic fibroblastoma involving the right elbow. (A) Sagittal T1WI, (B) sagittal T2WI with fat saturation, and (C) enhanced T1WI with fat saturation show a subcutaneous, well-circumscribed, oval mass in the elbow, and infiltration of the surrounding fat, superficial fascia. Both T1WI and T2WI reveal prominent low signal. Mild contrast enhancement is seen after intravenous administration of Gd-DTPA (arrows).

and more aggressive in their biologic behavior. There is a male predilection and almost 50% of patients are bilateral. Clinically, patients reveal firm subcutaneous nodules on the soles of the feet that are multiple in 33% of cases (36,38). Modified footwear is the commonly used therapy, so surgical treatment is not usually required (37). MR imaging typically reveals intermediate signal intensity mass with linear tails of extension along the plantar aponeurosis (*Figure* 7). Contrast enhancement is common after intravenous administration of contrast agent (38,39).

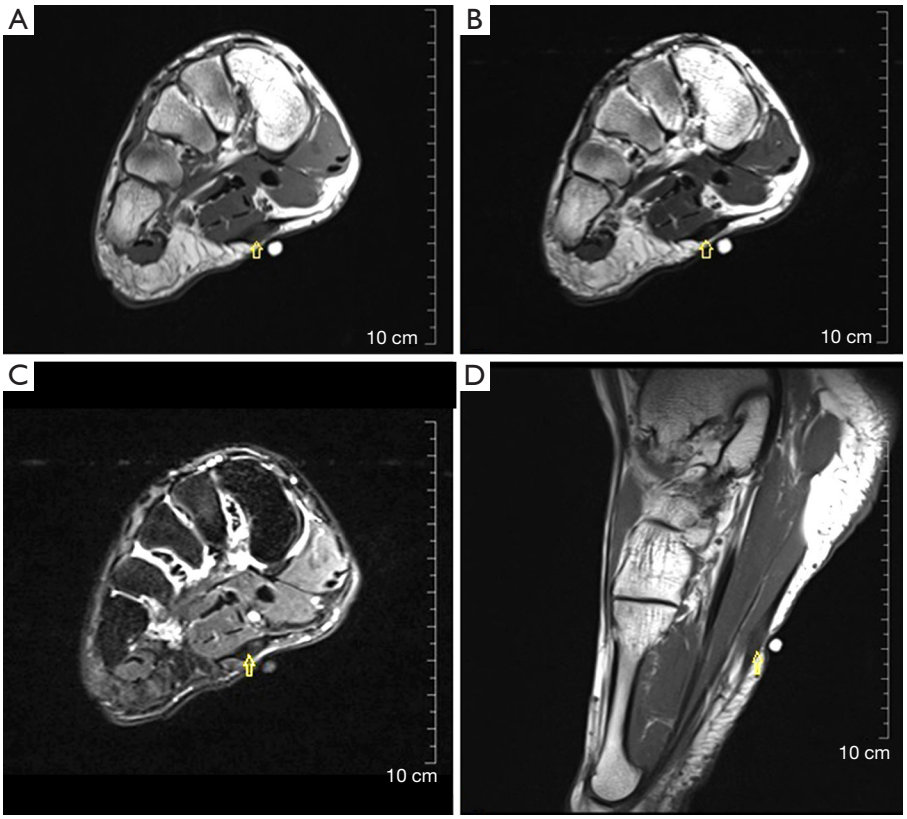

Figure 7 A 64-year-old man with plantar fibromatoses involving the right planta pedis. (A) Axial T1WI, (B) axial T2WI, (C) axial T2WI with fat saturation and (D) sagittal T1WI reveal a fusiform, intermediate signal intensity mass with linear tails of extension along the plantar aponeurosis (arrows).

Intermediate-rarely metastasizing fibroblastic/ myofibroblastic tumors

DFSP is a superficial, with low to intermediate grade malignant potential, locally aggressive fibroblastic neoplasm, which arises from the dermis and accounts for approximately 6% of all soft tissue sarcomas (40). The lesions are slowly growing, reddish-brown to bluish, firm, superficial nodules fixed to the skin (40,41). Lesions may be multiple, and small nodules may coalesce to form a plaque. Large lesions may invade underlying structures, ulcerate, bleed, or become painful. The lesion usually presents in young to middle-aged adult patients, with a slight male predominance. This subcutaneous mass most frequently involves the trunk and proximal upper and lower extremities, followed by the head and neck (41). At gross pathologic examination, this lesion is most commonly seen as a protuberant mass involving the subcutaneous tissue and skin with an average size of 5 cm. Local recurrence is common. Pathologically, the lesion is generally composed of a uniform population of fibroblasts, arranged in a distinct storiform pattern (40). Lesions may contain myxoid or densely collagenous regions (40).

Typical imaging manifestations of DFSP show a subcutaneous protuberant mass with a lobular or nodular architecture involving the skin and subcutaneous adipose tissue (*Figure 8*) (42). The boundary of lesions is often well-defined. CT or MR images are well suited to demonstrate this location and the distinct lobular or nodular architecture (43,44). More importantly, the relationship of the lesion to the underlying structures is well delineated. The intrinsic signal intensity of the lesion on MRI or the tissue attenuation on CT is nonspecific, which is similar to that of muscle. Fat-suppressed T2WI or STIR images typically demonstrate high signal intensity (43-45). Imaging may show heterogeneity compatible with hemorrhage and/or necrosis as seen pathologically within the lesion. Satellite nodules in the adjacent subcutaneous tissues may be seen on CT or MR imaging. Moderate to apparent

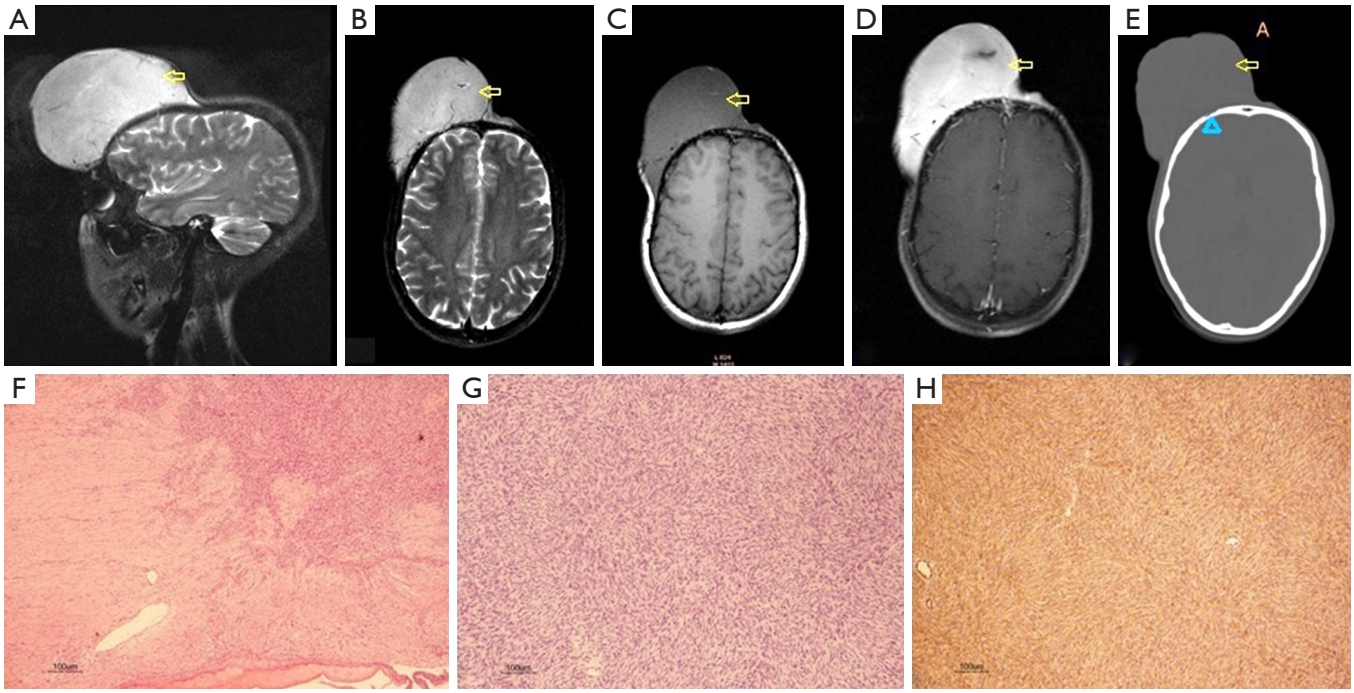

Figure 8 A 26-year-old female with recurrent DFSP of the frontal part. (A) Sagittal T2WI with fat suppression shows a large higher signal mass at site of previous resection, which protrudes through skin; (B) axial T2WI with fat suppression shows a large mass of uniform high signal; (C) axial T1WI displays intermediate signal intensity homogeneously; (D) after intravenous administration of gadolinium, axial T1WI with fat saturation shows apparent homogeneous enhancement in the mass (arrows). Axial CT image of bone window shows local bone destruction adjacent to the mass (arrow head); (F,G) histopathology photographs show monomorphous spindle-shaped cells arranged in a storiform pattern on a background of fibrous stroma (H&E, F, ×50; G, ×100); (H) immunohistochemical staining shows the spindle cells are positive for CD34 (original magnification, ×100).

homogeneous enhancement is usually seen after intravenous administration of contrast material, and some of which are detected linear extensions along the skin (42,45). Although imaging findings of DFSP is nonspecific, in our experience, linear extension along the skin surface is suggestive of the diagnosis. MRI is more useful in identifying the extent and depth of DFSP tumor infiltration than CT, facilitating preoperative planning for adequate margins and tumor clearance (42).

Pericytic/perivascular tumors

Glomus tumors, a kind of pericytic (perivascular) tumors, are mesenchymal neoplasms composing of cells resembling the modified smooth muscle cells of the normal glomus body. They are rare, accounting for less than 2% of soft tissue tumors, and usually locate about the terminal phalanx of the hand, followed by the wrist, forearm, and foot (46). Unusual sites affected include the thigh, stomach, nerve, lips, and face, etc. (47). Adults between 20 and 40 years of age are usually affected. Glomus tumors occur with equal frequency in men and women, except for subungual lesions, which are far more common in women (46). Multiple lesions are present in nearly 10% of patients, which is called glomangiomatosis (48). Clinically, the glomus tumor is seen as a small, red-blue, superficial nodule with symptoms of paroxysms of radiating pain, caused by temperature change or pressure. The classic clinical triad of pain, tenderness, and cold sensitivity is present in approximately 30% of patients (46,47). A soft tissue mass is seen on radiographs, located along the dorsal surface of the finger, either laterally or medially, related to the nail bed (49). In some cases, extrinsic erosion of bone, often with a sclerotic margin, can be seen. CT scanning reveals a nonspecific subungual soft tissue mass. MR imaging shows these lesions as small masses with very high signal intensity and homogeneity on T2WI. Lesions were typically homogeneously hyperintense and enhanced prominently and diffusely (*Figure 9*) (49,50).

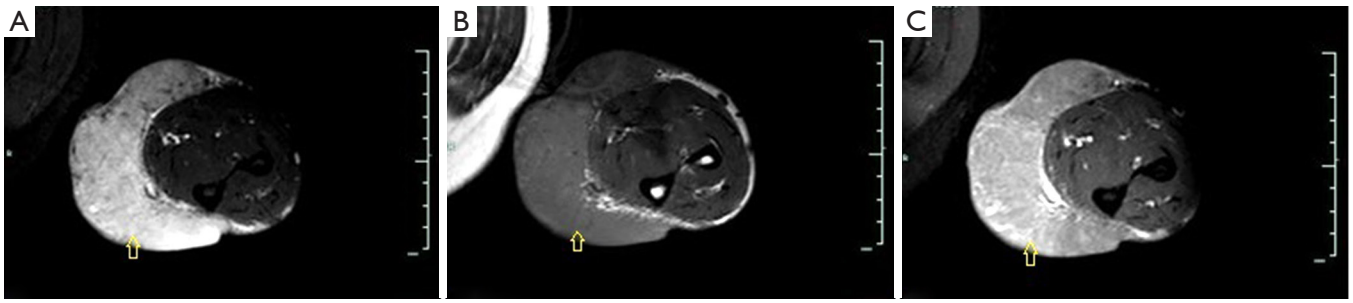

Figure 9 A 36-year-old male of glomus tumors with a palpable red mass in the left arm for about twenty years. (A) Axial T2WI with fat suppression shows a semi-round mass of uniform high signal along the subcutaneous tissue; (B) axial T1WI displays mildly high signal intensity homogeneously; (C) after intravenous administration of gadolinium, axial T1WI with fat suppression shows apparent homogeneous enhancement in the mass (arrows).

Vascular tumors

Vascular tumors are common soft tissue masses, particularly in young patients, frequently confused with other neoplastic masses both clinically and radiologically. However, CT and MR imaging often demonstrate characteristic features that allow imaging diagnosis (51). The most common entities of superficial vascular tumors include benign ones such as haemangioma, angiomatosis and lymphangioma, and malignancy such as angiosarcoma.

Benign vascular tumors

Hemangioma

Hemangiomas most frequently affect infancy and childhood. Soft tissue hemangiomas are usually discovered in the first three decades of life, with 30% discovered at birth (51). These lesions are more common in female with an approximate 3:1 ratio to male. Soft tissue hemangiomas may be superficial or deep. The latter lesions often involve intramuscular. Hemangiomas can be histologically classified as capillary, cavernous, arteriovenous, venous type by the predominant style of vascular channel identified within the lesion. Klippel-Trenaunay syndrome (KTS) is a rare congenital malformation characterized by a low-flow combined vascular malformation, including venous and lymphatic components in association with a cutaneous venular lesion which usually has a sharply demarcated, geographic distribution over the affected area, manifesting as a "port wine stain". There is typically overgrowth of the affected limb-limb hypertrophy. Nonvascular elements are also commonly present in hemangiomas, including fat, smooth muscle, fibrous tissue, and thrombus (51,52).

Capillary hemangioma

Capillary hemangioma is composed of small vessels lined by a flattened endothelium, which typically involve the skin and subcutaneous tissue. The juvenile variety is particularly common. Clinically juvenile hemangiomas are usually detected several weeks after birth and are enlarging, reaching their maximal size by 6 to 12 months of age. Lesions of hemangioma initially appear as a flat reddish macule that is similar to port-wine stain but its color will be intensified when crying or straining. Most of the juvenile hemangiomas subside spontaneously by 7 years of age. Although capillary hemangiomas are overall the most common type of angiomatous lesion, radiological evaluation is infrequent because they can be diagnosed clinically (51,52).

Cavernous hemangioma

Cavernous hemangioma is pathologically composed of dilated spaces filled with blood and lined by flattened endothelium. They often affect children and young adults. Cavernous hemangiomas present clinically as a nonspecific deep intramuscular mass. In unusual cases located superficially, lesions may reveal bluish skin discoloration. These lesions often present as a solitary purple well-defined mass on the trunk and are more common in women (51,52). Unlike capillary hemangiomas, cavernous lesions are often less well-circumscribed, and frequently require surgical resection. For these reasons, although cavernous hemangiomas are less common than the capillary variety, they are more frequently imaged by radiologists (51,52). Cavernous hemangiomas are usually calcification, typically containing dystrophic mineralization in organizing thrombus which is called phlebolith.

Imaging evaluation is mainly used to detect the vast majority of soft tissue hemangiomas which are deep-

Figure 10 A 58-year-old woman of hemangioma with a 10-year history of a slowly enlarging soft mass in the superficial proximal and lateral part of left calf. (A) Coronal T2-weighted image with fat saturation, (B) axial T2-weighted image with fat saturation, (C) coronal T1-weighted image, and (D) axial T1-weighted image show a fusiform subcutaneous heterogeneous mass. (E) Coronal T1-weighted image with fat suppression, and (F) axial T1-weighted image with fat suppression following intravenous gadolinium show prominent enhancement (arrows).

seated such as intramuscular lesions (53). Few imaging examinations for superficial soft tissue hemangiomas are described in the literature. As for capillary hemangiomas, superficial lesions (strawberry nevi) are typically easily diagnosed clinically with confidence, and if imaged, only staging with extent is required for appropriate patient management. This is in distinct contrast to cavernous lesions that are clinically nonspecific but usually reveal a pathognomonic MR imaging appearance.

Generally, radiographs are often normal or reveal only a nonspecific soft tissue mass. Non-enhanced CT often shows a poorly defined lesion of similar attenuation to that of skeletal muscle. Marked enhancement of the serpentine vascular components may be seen after intravenous administration of contrast medium (54). CT is the most sensitive modality to identify calcifications and phleboliths in the lesions (55,56). MR imaging is the best modality to evaluate soft tissue hemangiomas, which often show a poorly marginated mass of low-to-intermediate signal intensity on T1-weighted images (T1WI), and on T2-weighted images (T2WI) soft tissue hemangiomas reveal either a well-marginated or an infiltrative mass with very high signal intensity in areas of vascular components. Rather than displacing or destroying adjacent structures, they frequently tend to infiltrate adjacent tissue. Hemangiomas typically show prominent enhancement after intravenous administration of gadolinium (*Figure 10*) (54-56).

Lymphangioma

Lymphangioma is a benign, cavernous/cystic vascular lesion composed of dilated lymphatic channels, most frequent in the neck and axilla. Patients usually present at birth or by 2 years of age (51). Imaging findings may reflect the pathologic appearance with large, cystic spaces (57).

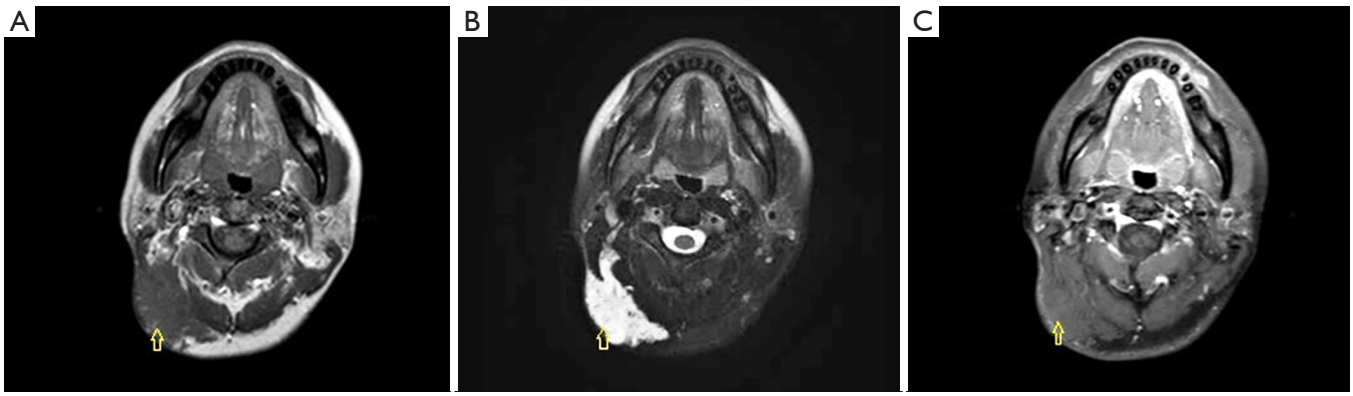

Figure 11 A 37-year-old female of lymphangioma presenting with a mass in the left side of the neck. (A) The lesion contains mostly low-intermediate signal on axial T1WI, and (B) mostly high signal separated by some low signal on axial T2WI with fat saturation; (C) after intravenous administration of Gd-DTPA, the lesion shows mild enhancement on axial T1WI with fat saturation (arrows).

CT shows a cystic lymphangioma as a unilocular or multilocular mass of water attenuation. Lesion walls and septa are typically of uniform thickness, and enhancement after intravenous contrast may be seen. Thicker septations are well delineated on CT. On T1WI, lymphangiomas show heterogeneous with low signal intensity, similar to or slightly less than that of muscle, and high signal intensity, greater than that of fat on T2WI, reflecting the preponderance of fluid-filled cystic spaces (*Figure 11*). Focal heterogeneity in the lesions is present in nearly all cases and appears as low-intensity linear structures of variable thickness representing fibrous septa (57,58).

Angiomatosis

Angiomatosis is a diffuse proliferation of benign, architecturally well-developed blood vessels that affects a large segment of the body in a contiguous fashion. About two thirds of cases of angiomatosis present in the first two decades of life. The more extensive the soft tissue involved, particularly visceral, the poorer the prognosis. Imaging of these lesions is identical to that of solitary hemangioma but much more extensive (59,60).

Malignant vascular tumors

Angiosarcoma is a malignant vascular tumor, and most frequently involves the skin and deep soft tissues (61). Approximately 40% of cases arise in the deep muscles of the lower extremities. Older patients are generally affected, and men are affected twice as commonly as women. Chronic lymphedema is a well-recognized predisposition to angiosarcoma (61). Angiosarcoma may also be radiation-induced (62,63). The intrinsic characteristics of angiosarcoma involving the skin and subcutaneous tissues are usually nonspecific on CT and MRI (64-66). Vascular channels and spaces are not typically apparent by imaging in these superficial lesions (67,68). Underlying manifestations of chronic lymphedema are frequently associated with angiosarcoma, including extremity enlargement, diffuse skin thickening, as well as thickening and edema of the subcutaneous connective tissue septae on CT and MR imaging (*Figure 12*) (64,65,67).

Nerve sheath tumors

Nerve sheath tumors are very common soft tissue tumors which arise from the nerve. Schwannoma and neurofibroma are the most common types of benign peripheral nerve sheath tumors (BPNSTs) (69), and malignant peripheral nerve sheath tumor (MPNST) accounts for 5% to 10% of all soft tissue sarcomas (70). Imaging characteristics often suggest neoplastic lesions of neurogenic origin.

Benign nerve sheath tumors

Schwannoma

Schwannoma, also called neurilemoma, is most commonly detected in patients between the ages of 20 and 50 years and occurs with equal frequency in men and women. Schwannomas are slightly less common than neurofibromas and comprise approximately 5% of all benign soft tissue tumors (69). Common sites are the cutaneous nerves of the

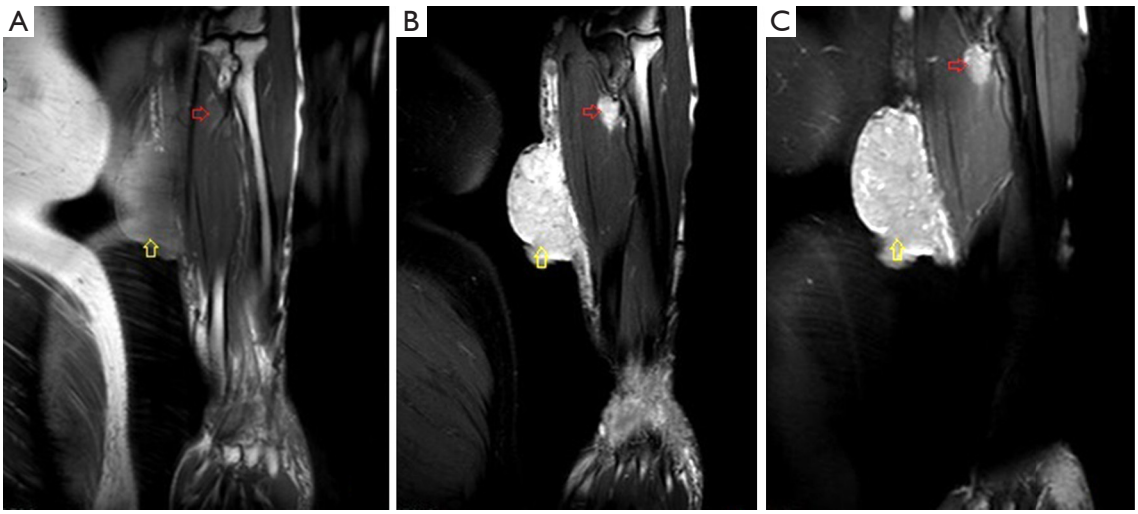

Figure 12 A 39-year-old man with angiosarcoma involving the medial forearm. (A) Coronal T1-weighted image and (B) T2-weighted image show a subcutaneous mass with prolonged T1 and T2 relaxation time in the superficial medial forearm, which invades the subcutaneous tissue (yellow arrows). A nodular mass is also found in the muscle of proximal arm at the level of radial tuberosity (red arrows); (C) after intravenous administration of Gd-DTPA, lesions show markedly enhancement on coronal T1WI with fat saturation.

head and neck, and the flexor surfaces of the extremities (71), particularly the peroneal and ulnar nerves (72). Affected nerve and tumor are separable within the epineurium. A schwannoma is almost invariably a slowly growing nonaggressive neoplasm that usually presents clinically as a painless mass, often smaller than 5 cm, without neurologic symptoms. Pain may be associated with large lesions (69). The histologic hallmark of schwannoma is the identification of Antoni A and Antoni B regions. Antoni A areas are more organized and are hypercellular composed of spindle cells arranged in short bundles or interlacing fascicles. Antoni B regions are hypocellular, less organized, and contain more myxoid, loosely arranged tissue, with high water content (73,74). Large schwannomas commonly undergo degenerative changes, including cyst formation, calcification, hemorrhage, and fibrosis (75). Surgical resection with sparing of the nerve is curative.

Neurofibroma

Neurofibroma most commonly affects patients 20 to 30 years of age and demonstrates no sex predilection. These lesions constitute slightly more than 5% of all benign soft tissue tumors (76,77). There are three types of neurofibromas, including localized, diffuse, and plexiform. The localized form accounts for approximately 90% of these lesions, and the vast majority is solitary and not associated with neurofibromatosis type 1 (NF-1) (78). Localized neurofibromas often affect superficial cutaneous nerves, which are slow-growing, usually smaller than 5 cm at presentation and painless. The diffuse neurofibroma primarily affects children and young adults and most frequently involves the subcutaneous tissues of the head and neck. Most of the diffuse neurofibromas are isolated papules and masses (76,78,79). Localized neurofibromas show a well-circumscribed fusiform shape, representing the mass with the entering and exiting nerve (77). Unlike schwannomas, neurofibromas are intimately intermixed and inseparable from normal nerve tissue on histopathology, which do not contain Antoni A and B regions (80). Neurofibromas cannot be separated from normal nerve, and complete excision of the neoplasm requires sacrifice of the nerve (76,77).

Malignant nerve sheath tumors

MPNST is a malignant nerve sheath tumor arising from a peripheral nerve, from a pre-existing benign nerve sheath tumor (usually neurofibroma) or in a patient with neurofibromatosis type 1 (70). MPNST is a rare tumor accounting for up to 5% of all soft tissue sarcomas, which typically affects patients aged 20 to 50 years (70). Up to 50% of MPNSTs are associated with neurofibromatosis type 1 (81). MPNST most commonly arises in the extremities, followed by the trunk and the head and neck area (70). The

Figure 13 A 56-year-old male of peripheral nerve sheath tumor with pain in the left arm for about two years. (A) Coronal T2WI with fat suppression shows a high signal mass of fusiform shape with entering and exiting nerve; (B) axial T2WI with fat suppression shows a round mass of uniform high signal, and (C) axial T1WI displays mildly high signal intensity homogeneously; (D) after intravenous administration of gadolinium, axial T1WI shows apparent homogeneous enhancement in the mass (arrows).

sciatic nerve is most frequently affected (70). There are no specific imaging features that distinguish MPNSTs from other high-grade sarcomas, except possible origin from a large nerve (82).

Imaging of nerve sheath tumors

Subcutaneous neurogenic neoplasms are often not imaged and have a nonspecific appearance (83). Generally, deep-seated neurogenic neoplasms usually have a diagnostic imaging appearance, particularly on MRI, including fusiform shape with entering and exiting nerve, target sign, split-fat sign, fascicular sign and associated muscle atrophy (83). In contradistinction, in superficial peripheral nerve sheath tumors (PNSTs), it is often difficult or impossible to identify this appearance, and imaging findings are nonspecific (83,84). However, these superficial lesions, as with other cutaneous or subcutaneous lesions, often are not imaged because of the so-called ease of clinical assessment (69,76).

MRI is superior to CT for demonstrating the virtually fusiform appearance of schwannoma, localized neurofibroma, and MPNST (84,85). On plain CT scans, PNSTs frequently have low attenuation, which is attributed to high lipid content of myelin from Schwann cells, presence or entrapment of fat, endoneurial myxoid tissue with high water content (Antoni B areas in schwannomas or myxoid areas in neurofibromas) (84,85). Heterogeneity may be seen in neurogenic neoplasms and is a more common feature of MPNST (83). On MR images, the signal intensity of neurogenic neoplasms is relatively nonspecific and is similar to or lower than that of muscle on T1WI and higher than that of fat on T2WI (*Figure 13*) (83-85).

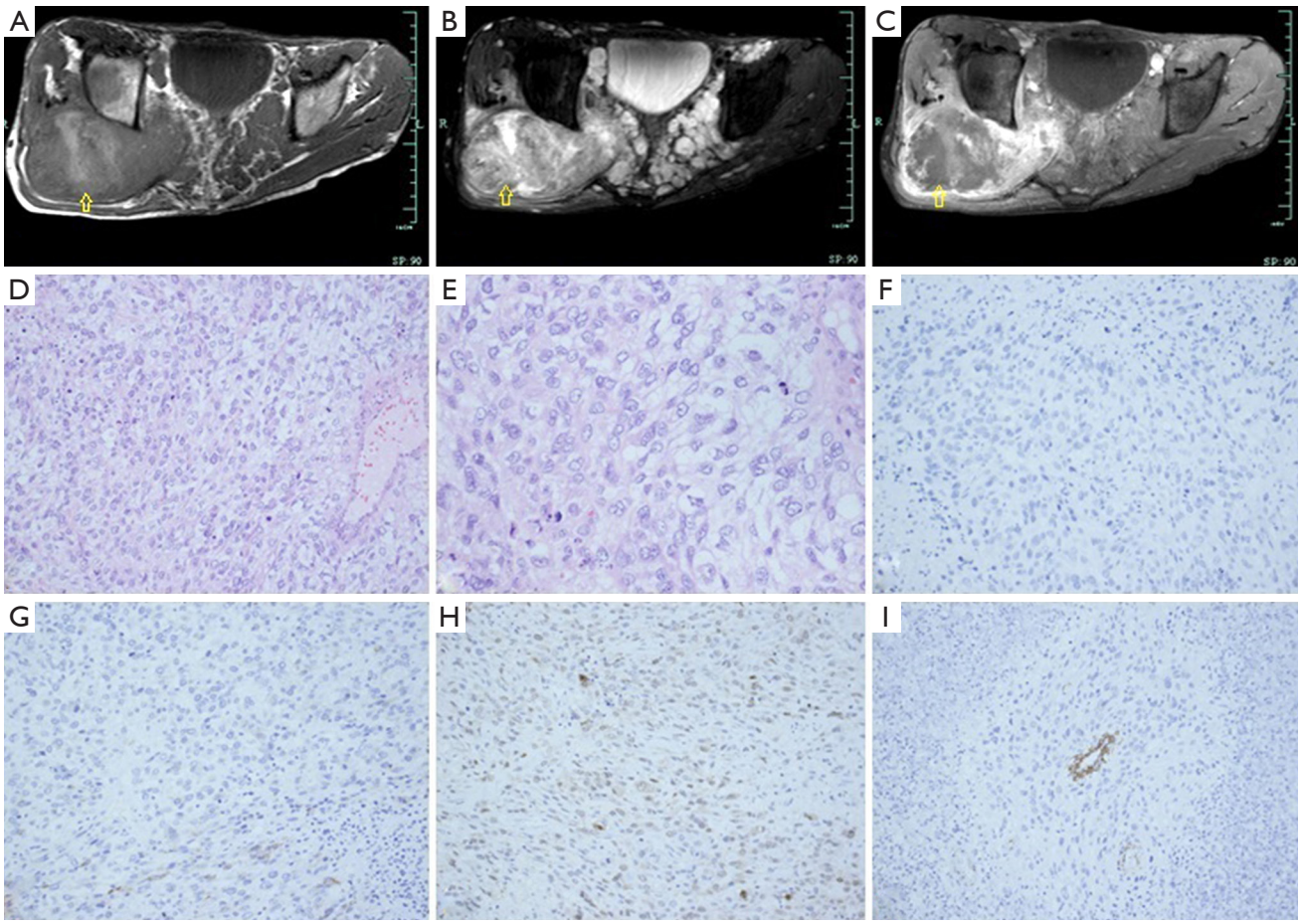

Figure 14 A 22-year-old man of malignant peripheral nerve sheath tumor with a rapid growing mass on the hip. (A) Axial T1WI of the hip shows irregular, ill-defined, heterogeneous mass with high and low signal intensity inside; (B) axial T2WI with fat saturation shows inhomogeneous high signal intensity inside the lesion, and lots of nodes locating through the nerve routes in the pelvic and subcutaneous; (C) axial post-contrast T1WI with fat suppression shows apparent inhomogeneous enhancement with lack of contrast in a necrotic center (arrows); (D,E) histopathology (H&E, D, ×200; E, ×400) of malignant peripheral nerve sheath tumor displays areas of necrosis with palisading of tumor cells and lots of nuclear division; (F-I) Immunohistochemistry stain of cytokeratin (F, ×200), epithelial membrane antigen (G, ×200), S100 (H, ×200) and smooth muscle antigen (I, ×200) shows no expression of cytokeratin and different expression of epithelial membrane antigen, S100, and smooth muscle antigen.

The target sign is described as being nearly pathognomonic of neurofibroma on T2WI and consists of low-to-intermediate signal intensity centrally, with a ring of high signal peripherally (86). Enhanced central areas with contrast strongly suggest a lesion is a BPNST as opposed to MPNST (*Figure 14*) (86-88). This kind of MRI finding corresponds pathologically to fibrous tissue (with high collagen content) centrally and more myxoid tissue peripherally (*Figure 15*) (85,86).

The margins of BPNSTs are usually well-defined on CT and MR images. Neurofibromas, despite being more common to extend beyond the epineurium, remain well-circumscribed in most cases, also causing a defined margin on imaging (84). However, indistinct margins are far more frequent in MPNSTs as a result of more infiltrative growth (82,83,88).

A rim of fat (split-fat sign) is often present about deep-seated neurogenic neoplasms and has been described previously on CT scans, despite being much easier to appreciate on T1-weighted MR images (89). Because the neurovascular bundle is surrounded by fat, masses arising in this site maintain a rim of fat about them as they slowly

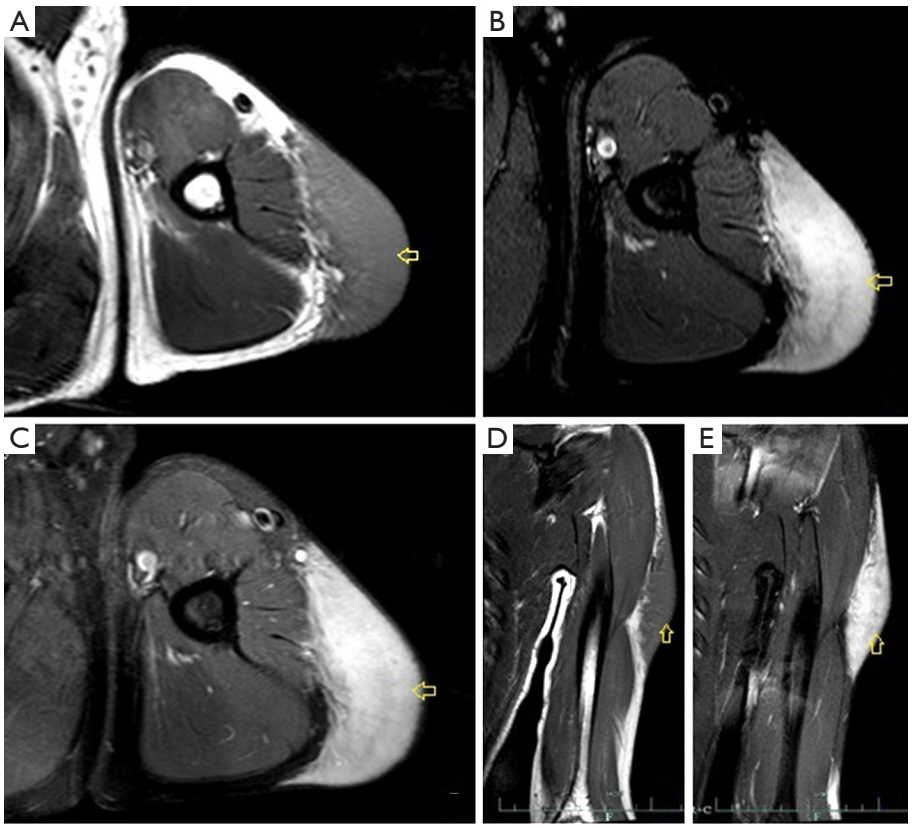

Figure 15 A 19-year-old male of neurofibroma presenting with a palpable mass in the left arm for over 6 years, and continuing growth. (A) Axial T1WI displays a mass of fusiform shape with mildly high signal intensity homogeneously along the subcutaneous tissue; (B) axial T2WI with fat suppression shows uniform high signal; (C) after intravenous administration of gadolinium, axial T1WI shows apparent homogeneous enhancement in the mass; (D) coronal T1WI and (E) contrast enhanced T1WI with fat suppression show similar signal to the axial images (arrows).

enlarge (89). The split-fat sign is more common in BPNST and lesions of large nerves. MPNST less frequently demonstrates a complete fat rim, reflecting its more infiltrative growth pattern (84,88,89).

Differentiation of BPNST from MPNST is often very difficult (82,84,88,90). However, imaging features favoring malignancy include size larger than 5 cm, prominent enhancement, marked heterogeneity with central necrosis, rapid growth, and infiltrative margins in a non-plexiform lesion (88). Recognition of these imaging features is important for prospective diagnosis and to help guide therapy in the clinical management of these patients (88).

Undifferentiated/unclassified sarcomas

This new category, which may comprise up to 20% of all pleomorphic soft tissue sarcomas, encompasses tumors in which all recognizable lines of differentiation have been excluded. These tumors are typically high grade, show a wide range of morphological features, and are often associated with a poor prognosis. These tumors can be subclassified as round cell, spindle cell, pleomorphic, and epithelioid according to predominant morphological patterns.

Undifferentiated pleomorphic sarcoma (UPS), previously called malignant fibrous histiocytoma, is the most common soft tissue sarcoma of late adult life, accounting for 20% to 30% of all soft tissue sarcomas (91-93). The peak incidence is in the fifth decade with a range of 10 to 90 years of age, and most patients are between 50 and 70 years of age. Men account for 70% of lesions. The most commonly affected sites are extremities, the lower extremity accounts for 50% of all cases (particularly the thigh) (92). Most of UPS are usually deep intramuscular lesions. Only 5% to 10% of UPS involve the subcutaneous tissue (91-93). Clinically, patients present

Figure 16 A 74-year-old male of undifferentiated pleomorphic sarcoma presenting with a palpable mass in the right lateral superficial calf for several years. (A) Axial T1WI displays a superficial fusiform mass with intermediate signal similar to the adjacent muscles in the right calf; (B) axial T2WI with fat saturation shows moderate high signal in the lesion with adjacent skin thickened; (C) after intravenous administration of gadolinium, axial T1WI with fat saturation shows apparent homogeneous enhancement in the mass; (D) coronal enhanced T1WI with fat saturation shows similar signal to the axial image, and the lesion extends to adjacent cutaneous and subcutaneous tissue as well (arrows).

with an enlarging, painless, soft tissue mass. Subcutaneous lesions are usually much smaller. Storiform/pleomorphic subtype is the most common type in UPS (91,93).

Subcutaneous UPS reveals an intrinsically nonspecific soft tissue mass replacing the normal subcutaneous fat on CT, or MR images (94,95). These patients frequently present earlier than those with deep-seated lesions. The small initial lesion size frequently suggests a benign diagnosis to both radiologists and clinicians, leading to inappropriate marginal excision and local recurrence (94). These lesions commonly invade the underlying muscle and may cause overlying skin ulceration (92). CT scans demonstrate UPS as lobulated soft tissue masses of similar attenuation to muscle. Areas of decreased attenuation frequently are apparent within the mass more centrally, corresponding to myxoid regions or necrosis (94). MR images often show heterogeneous signal intensity on all pulse sequences, which depends on variable amount of collagen, myxoid tissue, necrosis, and hemorrhage, and may be predominantly high or low signal intensity on T2WI (95). Tumor margins are usually relatively well-defined because of pseudocapsule. Solid components of UPS typically show enhancement after intravenous administration of contrast agent (*Figure 16*) (94,95).

Conclusions

In comparison with a large number of benign lesions that may be seen in the superficial tissue, malignancies arising from the cutaneous and subcutaneous tissue are relatively uncommon. The imaging appearance of a superficial mass often yields limited information to help narrow the differential diagnosis. Therefore, not only the imaging appearance but also the lesion location and the patient's age should be considered when evaluating a superficial mass.

Ultrasound is often the first examination used as it is simple and convenient, and sometimes to guide the needle biopsy. However, it is operator-dependent and non-specific. A radiograph is useful to rule out a bone tumor invading the soft tissues. CT is mainly used to detect calcifications and bone erosion which could not be seen on radiographs. MRI is the preferred modality for evaluating soft tissue lesions, which is by far superior to CT and provides higher soft tissue contrast. Additionally, MRI allows multi-planar and multi-parameter image acquisition, and obviates the need for iodinated contrast agents or for ionizing radiation. MRI is able to accurately define the relationship of tumors to adjacent structures and compartments in multiple planes. When a lesion has a nonspecific MR imaging appearance, it is useful to formulate a suitably ordered differential diagnosis on tumor prevalence, patient age, and lesion anatomic location. Differential can be refined by considering clinical history and diagnostic radiological features. Additionally, imaging can help make a strategy for therapy, such as preoperative planning of the extent of surgery and adjuvant chemotherapy/radiotherapy.

Acknowledgements

We thank Dr. Liang Qi, from Department of Radiology, Jiangsu Province Hospital, for help to collect materials.
Funding: This study was supported by a grant from Project co-sponsored by Zhejiang Province and Health & Family Planning Commission of China (WSK 2014-2-009).

Footnote

Conflicts of Interest: The authors have no conflicts of interest to declare.

References

1. Morris CJ, Younan Y, Singer AD, Johnson G, Chamieh J, Datir A. Masses of the hand and wrist, a pictorial review. Clin Imaging;40:650-65.
2. Rimondi E, Benassi MS, Bazzocchi A, Balladelli A, Facchini G, Rossi G, Taieb S, Vanel D. Translational research in diagnosis and management of soft tissue tumours. Cancer Imaging 2016;16:13.
3. Caracciolo JT, Letson GD. Radiologic approach to bone and soft tissue sarcomas. Surg Clin North Am 2016;96:963-76.
4. Zhuang KD, Tandon AA, Ho BC, Chong BK. MRI features of soft-tissue lumps and bumps. Clin Radiol 2014;69:e568-83.
5. Chung WJ, Chung HW, Shin MJ, Lee SH, Lee MH, Lee JS, Kim MJ, Lee WK. MRI to differentiate benign from malignant soft-tissue tumours of the extremities: a simplified systematic imaging approach using depth, size and heterogeneity of signal intensity. Br J Radiol 2012;85:e831-6.
6. Beaman FD, Kransdorf MJ, Andrews TR, Murphey MD, Arcara LK, Keeling JH. Superficial soft-tissue masses: analysis, diagnosis, and differential considerations. Radiographics 2007;27:509-23.
7. Costigan DC, Doyle LA. Advances in the clinicopathological and molecular classification of cutaneous mesenchymal neoplasms. Histopathology 2016;68:776-95.
8. Morel M, Taieb S, Penel N, Mortier L, Vanseymortier L, Robin YM, Gosset P, Cotten A, Ceugnart L. Imaging of the most frequent superficial soft-tissue sarcomas. Skeletal Radiol 2011;40:271-84.
9. Wu JS, Hochman MG. Soft-tissue tumors and tumorlike lesions: a systematic imaging approach. Radiology 2009;253:297-316.
10. Szyszko TA, Cook GJR. PET/CT and PET/MRI in head and neck malignancy. Clin Radiol 2018;73:60-9.
11. Sheikhbahaei S, Marcus C, Hafezi-Nejad N, Taghipour M, Subramaniam R. Value of FDG PET/CT in patient management and outcome of skeletal and soft tissue sarcomas. PET Clin 2015;10:375-93.
12. Erfanian Y, Grueneisen J, Kirchner J, Wetter A, Podleska L, Bauer S, Poeppel T, Forsting M, Herrmann K, Umutlu L. Integrated 18F-FDG PET/MRI compared to MRI alone for identification of local recurrences of soft tissue sarcomas: a comparison trial. Eur J Nucl Med Mol Imaging 2017;44:1823-31.
13. Partovi S, Chalian M, Fergus N, Kosmas C, Zipp L, Mansoori B, Ros P, Robbin M. Magnetic resonance/positron emission tomography (MR/PET) oncologic

applications: bone and soft tissue sarcoma. Semin Roentgenol. Semin Roentgenol 2014;49:345-52.
14. Mentzel T. Cutaneous lipomatous neoplasms. Semin Diagn Pathol 2001;18:250-7.
15. Nguyen T, Zuniga R. Skin conditions: benign nodular skin lesions. FP Essent 2013;407:24-30.
16. Coran A, Ortolan P, Attar S, Alberioli E, Perissinotto E, Tosi AL, Montesco MC, Rossi CR, Tropea S, Rastrelli M, Stramare R. Magnetic resonance imaging assessment of lipomatous soft-tissue tumors. In Vivo 2017;31:387-95.
17. Murphey MD, Carroll JF, Flemming DJ, Pope TL, Gannon FH, Kransdorf MJ. From the archives of the AFIP: benign musculoskeletal lipomatous lesions. Radiographics 2004;24:1433-66.
18. Nassif NA, Tseng W, Borges C, Chen P, Eisenberg B. Recent advances in the management of liposarcoma. F1000Res 2016;5:2907.
19. Weiss SW. Lipomatous tumors. Monogr Pathol 1996;38:207-39.
20. Gupta P, Potti TA, Wuertzer SD, Lenchik L, Pacholke DA. Spectrum of fat-containing soft-tissue masses at MR imaging: the common, the uncommon, the characteristic, and the sometimes confusing. Radiographics 2016;36:753-66.
21. Rizer M, Singer AD, Edgar M, Jose J, Subhawong TK. The histological variants of liposarcoma: predictive MRI findings with prognostic implications, management, follow-up, and differential diagnosis. Skeletal Radiol 2016;45:1193-204.
22. Lai FM, Lam WY. Nodular fasciitis of the dermis. J Cutan Pathol 1993;20:66-9.
23. Kumar E, Patel NR, Demicco EG, Bovee JV, Olivera AM, Lopez-Terrada DH, Billings SD, Lazar AJ, Wang WL. Cutaneous nodular fasciitis with genetic analysis: a case series. J Cutan Pathol 2016;43:1143-9.
24. Lu L, Lao IW, Liu X, Yu L, Wang J. Nodular fasciitis: a retrospective study of 272 cases from China with clinicopathologic and radiologic correlation. Ann Diagn Pathol 2015;19:180-5.
25. Kim ST, Kim HJ, Park SW, Baek CH, Byun HS, Kim YM. Nodular fasciitis in the head and neck: CT and MR imaging findings. AJNR Am J Neuroradiol 2005;26:2617-23.
26. Khuu A, Yablon CM, Jacobson JA, Inyang A, Lucas DR, Biermann JS. Nodular fasciitis: characteristic imaging features on sonography and magnetic resonance imaging. J Ultrasound Med 2014;33:565-73.
27. Rhee SJ, Ryu JK, Kim JH, Lim SJ. Nodular fasciitis of the breast: two cases with a review of imaging findings. Clin Imaging 2014;38:730-3.
28. Thompson LD. Elastofibroma. Ear Nose Throat J 2017;96:160.
29. Daghfous A, Bouzaidi K, Affes M, Ben Rhouma N, Rezgui Marhoul L. Dorsal elastofibroma: usefulness of MRI imaging. Tunis Med 2014;92:354-5.
30. Clinckemaillie G, Larbi A, Omoumi P, Manelfe J, Dallaudiere B. Bilateral elastofibroma dorsi: typical CT and MRI features. JBR-BTR 2014;97:45.
31. Abe S, Miyata N, Yamamoto Y, Yamaguchi T, Tamakawa M. Elastofibroma dorsi: CT, MRI, and pathologic findings. Plast Reconstr Surg 1999;104:2121-6.
32. Watanabe H, Ishida Y, Nagashima K, Makino T, Norisugi O, Shimizu T. Desmoplastic fibroblastoma (collagenous fibroma). J Dermatol 2008;35:93-7.
33. Singh NG, Mannan AA, Kahvic M. Desmoplastic fibroblastoma (collagenous fibroma): report of a case. Indian J Pathol Microbiol 2011;54:206-7.
34. Bonardi M, Zaffarana VG, Precerutti M. US and MRI appearance of a collagenous fibroma (desmoplastic fibroblastoma) of the shoulder. J Ultrasound 2013;17:53-6.
35. Shuto R, Kiyosue H, Hori Y, Miyake H, Kawano K, Mori H. CT and MR imaging of desmoplastic fibroblastoma. Eur Radiol 2002;12:2474-6.
36. Fetsch JF, Laskin WB, Miettinen M. Palmar-plantar fibromatosis in children and preadolescents: a clinicopathologic study of 56 cases with newly recognized demographics and extended follow-up information. Am J Surg Pathol 2005;29:1095-105.
37. Laskin WB, Miettinen M, Fetsch JF. Infantile digital fibroma/fibromatosis: a clinicopathologic and immunohistochemical study of 69 tumors from 57 patients with long-term follow-up. Am J Surg Pathol 2009;33:1-13.
38. Walker EA, Petscavage JM, Brian PL, Logie CI, Montini KM, Murphey MD. Imaging features of superficial and deep fibromatoses in the adult population. Sarcoma 2012;2012:215810.
39. English C, Coughlan R, Carey J, Bergin D. Plantar and palmar fibromatosis: characteristic imaging features and role of MRI in clinical management. Rheumatology (Oxford) 2012;51:1134-6.
40. Thway K, Noujaim J, Jones RL, Fisher C. Dermatofibrosarcoma protuberans: pathology, genetics, and potential therapeutic strategies. Ann Diagn Pathol 2016;25:64-71.
41. Acosta AE, Velez CS. Dermatofibrosarcoma protuberans. Curr Treat Options Oncol 2017;18:56.
42. Al Barwani AS, Taif S, Al Mazrouai RA, Al Muzahmi KS,

Alrawi A. Dermatofibrosarcoma protuberans: insights into a rare soft tissue tumor. J Clin Imaging Sci 2016;6:16.
43. Kransdorf MJ, Meis-Kindblom JM. Dermatofibrosarcoma protuberans: radiologic appearance. AJR Am J Roentgenol 1994;163:391-4.
44. Torreggiani WC, Al-Ismail K, Munk PL, Nicolaou S, O'Connell JX, Knowling MA. Dermatofibrosarcoma protuberans: MR imaging features. AJR Am J Roentgenol 2002;178:989-93.
45. Zhang L, Liu QY, Cao Y, Zhong JS, Zhang WD. Dermatofibrosarcoma protuberans: computed tomography and magnetic resonance imaging findings. Medicine (Baltimore) 2015;94:e1001.
46. Longhurst WD, Khachemoune A. An unknown mass: the differential diagnosis of digit tumors. Int J Dermatol 2015;54:1214-25.
47. Temiz G, Sirinoglu H, Demirel H, Yesiloglu N, Sarici M, Filinte GT. Extradigital Glomus Tumor Revisited: Painful Subcutaneous Nodules Located in Various Parts of the Body. Indian J Dermatol 2016;61:118.
48. Park EA, Hong SH, Choi JY, Lee MW, Kang HS. Glomangiomatosis: magnetic resonance imaging findings in three cases. Skeletal Radiol 2005;34:108-11.
49. Kim DH. Glomus tumor of the finger tip and MRI appearance. Iowa Orthop J 1999;19:136-8.
50. Dahlin LB, Besjakov J, Veress B. A glomus tumour: classic signs without magnetic resonance imaging findings. Scand J Plast Reconstr Surg Hand Surg 2005;39:123-5.
51. Abernethy LJ. Classification and imaging of vascular malformations in children. Eur Radiol 2003;13:2483-97.
52. Burrows PE, Laor T, Paltiel H, Robertson RL. Diagnostic imaging in the evaluation of vascular birthmarks. Dermatol Clin 1998;16:455-88.
53. Merrow AC, Gupta A, Adams DM. Additional imaging features of intramuscular capillary-type hemangioma: the importance of ultrasound. Pediatr Radiol 2014;44:1472-4.
54. Campione E, Diluvio L, Terrinoni A, Di Stefani A, Orlandi A, Chimenti S, Bianchi L. Progressive late-onset of cutaneous angiomatosis as possible sign of cerebral cavernous malformations. Dermatol Online J 2013;19:2.
55. Curé JK. Imaging of vascular lesions of the head and neck. Facial Plast Surg Clin North Am 2001;9:525-49.
56. Grippaudo FR, Piane M, Amoroso M, Longo B, Penco S, Chessa L, Giubettini M, Santanelli F. Cutaneous venous malformations related to KRIT1 mutation: case report and literature review. J Mol Neurosci 2013;51:442-5.
57. McAlvany JP, Jorizzo JL, Zanolli D, Auringer S, Prichard E, Krowchuk DP, Turner S. Magnetic resonance imaging in the evaluation of lymphangioma circumscriptum. Arch Dermatol 1993;129:194-7.
58. Lohrmann C, Foeldi E, Langer M. Diffuse lymphangiomatosis with genital involvement--evaluation with magnetic resonance lymphangiography. Urol Oncol 2011;29:515-22.
59. Mekhail Y, Prather A, Hanna C, Rosa M, Weinfurtner RJ. Focal angiomatosis of the breast with MRI and histologic features. Radiol Case Rep 2017;12:219-22.
60. Aronniemi J, Lohi J, Salminen P, Vuola P, Lappalainen K, Pitkaranta A, Pekkola J. Angiomatosis of soft tissue as an important differential diagnosis for intramuscular venous malformations. Phlebology 2017;32:474-81.
61. Young RJ, Brown NJ, Reed MW, Hughes D, Woll PJ. Angiosarcoma. Lancet Oncol 2010;11:983-91.
62. Chesebro AL, Chikarmane SA, Gombos EC, Giardino AA. Radiation-associated angiosarcoma of the breast: what the radiologist needs to know. AJR Am J Roentgenol 2016;207:217-25.
63. Brenn T, Fletcher CD. Radiation-associated cutaneous atypical vascular lesions and angiosarcoma: clinicopathologic analysis of 42 cases. Am J Surg Pathol 2005;29:983-96.
64. Gaballah AH, Jensen CT, Palmquist S, Pickhardt PJ, Duran A, Broering G, Elsayes KM. Angiosarcoma: clinical and imaging features from head to toe. Br J Radiol 2017;90:20170039.
65. Patt JC, Haines N. Soft tissue sarcomas in skin: presentations and management. Semin Oncol 2016;43:413-8.
66. Linda DD, Harish S, Alowami S, DeNardi F, Deheshi BM. Radiology-pathology conference: cutaneous angiosarcoma of the leg. Clin Imaging 2013;37:602-7.
67. Sanders LM, Groves AC, Schaefer S. Cutaneous angiosarcoma of the breast on MRI. AJR Am J Roentgenol 2006;187:W143-6.
68. Chopra S, Ors F, Bergin D. MRI of angiosarcoma associated with chronic lymphoedema: Stewart Treves syndrome. Br J Radiol 2007;80:e310-3.
69. Rodríguez-Peralto JL, Riveiro-Falkenbach E, Carrillo R. Benign cutaneous neural tumors. Semin Diagn Pathol 2013;30:45-57.
70. Luzar B, Falconieri G. Cutaneous Malignant Peripheral Nerve Sheath Tumor. Surg Pathol Clin 2017;10:337-43.
71. Adani R, Tarallo L, Mugnai R, Colopi S. Schwannomas of the upper extremity: analysis of 34 cases. Acta Neurochir (Wien) 2014;156:2325-30.
72. Strowd RE, Strowd LC, Blakeley JO. Cutaneous

manifestations in neuro-oncology: clinically relevant tumor and treatment associated dermatologic findings. Semin Oncol 2016;43:401-7.
73. Kurtkaya-Yapicier O, Scheithauer B, Woodruff JM. The pathobiologic spectrum of Schwannomas. Histol Histopathol 2003;18:925-34.
74. Argenyi ZB. Recent developments in cutaneous neural neoplasms. J Cutan Pathol 1993;20:97-108.
75. Xu SY, Sun K, Xie HY, Zhou L, Zheng SS, Wang WL. Hemorrhagic, calcified, and ossified benign retroperitoneal schwannoma: First case report. Medicine (Baltimore) 2016;95:e4318.
76. Ferner RE. The neurofibromatoses. Pract Neurol 2010;10:82-93.
77. Ferner RE. Neurofibromatosis 1 and neurofibromatosis 2: a twenty first century perspective. Lancet Neurol 2007;6:340-51.
78. Lu-Emerson C, Plotkin SR. The Neurofibromatoses. Part 1: NF1. Rev Neurol Dis 2009;6:E47-53.
79. Korf BR. Neurofibromatosis. Handb Clin Neurol 2013;111:333-40.
80. Abbas O, Bhawan J. Cutaneous plexiform lesions. J Cutan Pathol 2010;37:613-23.
81. Suresh K, Kliot T, Piunti A, Kliot M. Epigenetic mechanisms drive the progression of neurofibromas to malignant peripheral nerve sheath tumors. Surg Neurol Int 2016;7:S797-S800.
82. Kim A, Stewart DR, Reilly KM, Viskochil D, Miettinen MM, Widemann BC. Malignant peripheral nerve sheath tumors state of the science: leveraging clinical and biological insights into effective therapies. Sarcoma 2017;2017:7429697.
83. Chatzistefanou A, Mantatzis M, Deftereos S, Mintzopoulou P, Prassopoulos P. Peripheral nerve sheath tumors. Benign or malignant? The role of MRI and ultrasonography in a case report. J Neuroimaging 2014;24:308-10.
84. Verstraete KL, Achten E, De Schepper A, Ramon F, Parizel P, Degryse H, Dierick AM. Nerve sheath tumors: evaluation with CT and MR imaging. J Belge Radiol 1992;75:311-20.
85. Pilavaki M, Chourmouzi D, Kiziridou A, Skordalaki A, Zarampoukas T, Drevelengas A. Imaging of peripheral nerve sheath tumors with pathologic correlation: pictorial review. Eur J Radiol 2004;52:229-39.
86. Ghosh PS, Ghosh D. Teaching neuroimages: MRI "target sign" and neurofibromatosis type 1. Neurology 2012;78:e63.
87. Bhargava R, Parham DM, Lasater OE, Chari RS, Chen G, Fletcher BD. MR imaging differentiation of benign and malignant peripheral nerve sheath tumors: use of the target sign. Pediatr Radiol 1997;27:124-9.
88. Li CS, Huang GS, Wu HD, Chen WT, Shih LS, Lii JM, Duh SJ, Chen RC, Tu HY, Chan WP. Differentiation of soft tissue benign and malignant peripheral nerve sheath tumors with magnetic resonance imaging. Clin Imaging 2008;32:121-7.
89. Abreu E, Aubert S, Wavreille G, Gheno R, Canella C, Cotten A. Peripheral tumor and tumor-like neurogenic lesions. Eur J Radiol 2013;82:38-50.
90. Wasa J, Nishida Y, Tsukushi S, Shido Y, Sugiura H, Nakashima H, Ishiguro N. MRI features in the differentiation of malignant peripheral nerve sheath tumors and neurofibromas. AJR Am J Roentgenol 2010;194:1568-74.
91. Soleymani T, Tyler Hollmig S. Conception and management of a poorly understood spectrum of dermatologic neoplasms: atypical fibroxanthoma, pleomorphic dermal sarcoma, and undifferentiated pleomorphic sarcoma. Curr Treat Options Oncol 2017;18:50.
92. Clarke LE. Fibrous and fibrohistiocytic neoplasms: an update. Dermatol Clin 2012;30:643-56, vi.
93. Henderson MT, Hollmig ST. Malignant fibrous histiocytoma: changing perceptions and management challenges. J Am Acad Dermatol 2012;67:1335-41.
94. Fanburg-Smith JC, Spiro IJ, Katapuram SV, Mankin HJ, Rosenberg AE. Infiltrative subcutaneous malignant fibrous histiocytoma: a comparative study with deep malignant fibrous histiocytoma and an observation of biologic behavior. Ann Diagn Pathol 1999;3:1-10.
95. Galant J, Marti-Bonmati L, Soler R, Saez F, Lafuente J, Bonmati C, Gonzalez I. Grading of subcutaneous soft tissue tumors by means of their relationship with the superficial fascia on MR imaging. Skeletal Radiol 1998;27:657-63.

Cite this article as: Zhang J, Li Y, Zhao Y, Qiao J. CT and MRI of superficial solid tumors. Quant Imaging Med Surg 2018;8(2):232-251. doi: 10.21037/qims.2018.03.03

